Self-Generated Unconscious Processing of Loss Linked to Less Severe Grieving

Supplemental Information

MRI

Blood-oxygen-level dependent (BOLD) images were acquired on a GE 3-T scanner parallel to the anterior commissure-posterior commissure (AC-PC) line with a T2*-weighted EPI sequence of 45 contiguous slices (TR=2000ms, TE=25ms, flip angle = 77, FoV=192 x 192mm) of 3mm thickness and 3x3 in-plane resolution. Structural images were acquired with a T1-weighted SPGR sequence recording 256 slices at a slice thickness of 1mm and in-plane resolution of 1x1mm.

Preprocessing was carried out using FSL version 6 (FMRIB's Software Library, www.fmrib.ox.ac.uk/fsl) (1). Preprocessing included slice time correction, motion correction, skull stripping and smoothing with a Gaussian kernel of 6mm FWHM. A 120-second high pass filter was applied to the data. All data were corrected for head motion by removing the influence of six motion time courses. Bias field correction was implemented using FSL-FAST for functional and structural images (2). Following preprocessing functional images were registered to structural images with 7-degrees of freedom and then structural images were warped to the standard MNI space using a 12-degree affine registration followed by a non-linear warp implemented in FNIRT (3, 4). Following the acquisition of the first 23 subjects, the T1 bias corrections step failed necessitating the removal of this step from preprocessing for subsequent subjects. To reduce the effect of this noise on the overall model, these subjects were excluded from the pattern-training phase (i.e. Stroop task) and only incorporated in the pattern application phase (SART-PROBES). The primary analysis was run with and without these subjects and effects were unchanged (see Results). All images were registered to the MNI standard space template. All regional delineations are defined according to the Harvard-Oxford atlases.

MVPA analysis

The prediction of RT was implemented through a multivariate linear regression. For each subject, we first computed the z score of RT and the z score of the BOLD activity at each voxel within the feature mask across all deceased-related trials. Then we concatenated RT and BOLD activity across all subjects and constructed a linear regression model implemented using FaSTGLZ (5) to predict RT to deceased-related words using the BOLD activity across voxels in the d-SA voxel mask. A 10x10 fold cross validation procedure was used to optimize the neural pattern for d-SA (i.e. *W).* That is, the blocks were randomly split into 10 parts (folds), where nine folds were used to train the models, and the tenth fold was used to measure the out-of-sample prediction.

To test the significance of the prediction, we used a permutation procedure where we randomly permuted the RT and calculated the mean squared error (MSE) of the prediction. This procedure was repeated for 1000 times to obtain an empirical null distribution of the MSE. The significance of the prediction was then determined by comparing the observed MSE against the empirical null distribution.

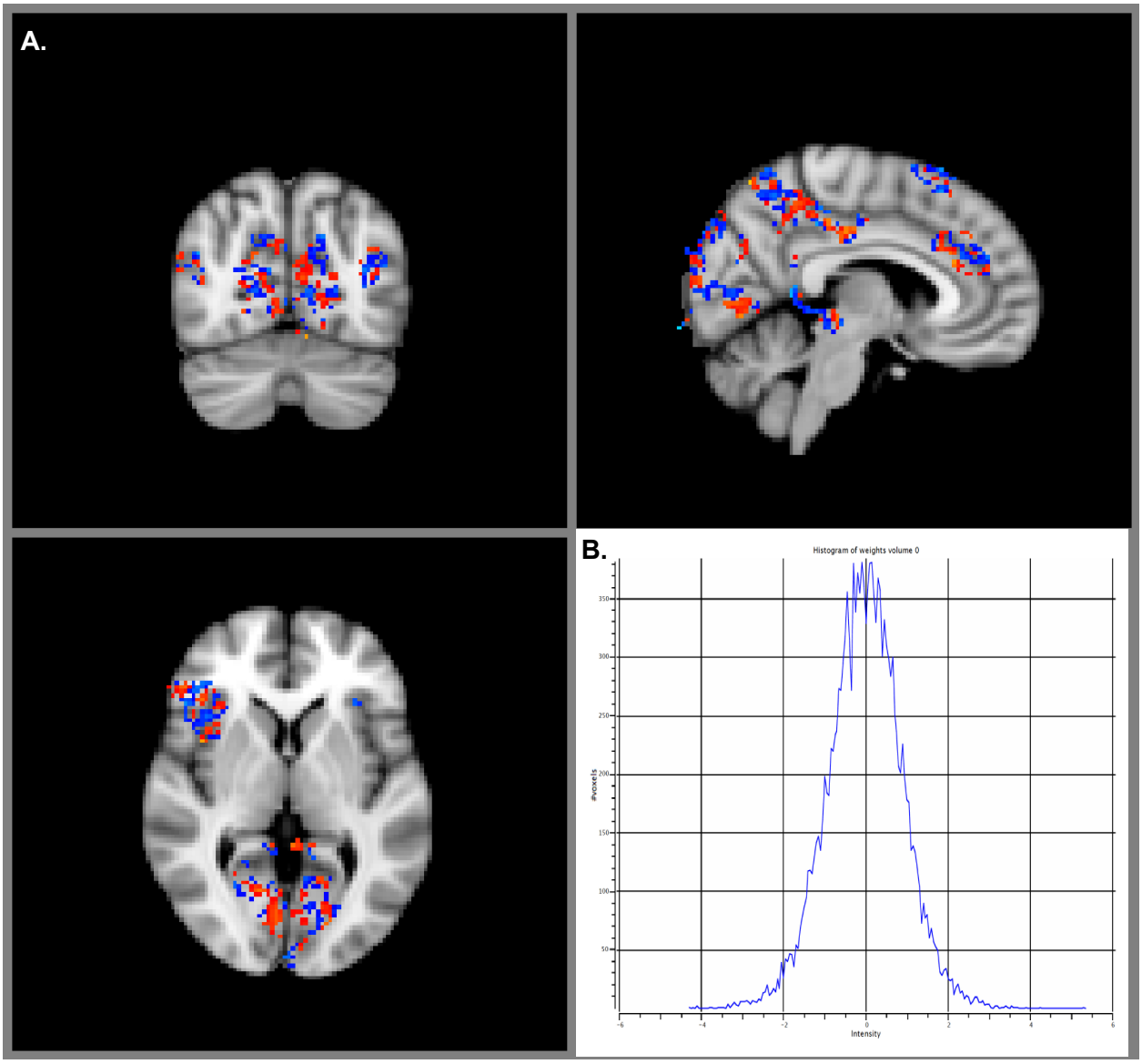

Figure S1. d-SA Weighting Matrix. A 3D weighting matrix was identified by the machine learning regression. This weighting matrix optimized the prediction of longer Stroop RTs on the basis of trial by trial BOLD data. Because it predicted longer Stroop RTs this matrix was interpreted as a neural pattern corresponding to the engagement of deceased-related selective attention (i.e. d-SA), which when applied in the Stroop task would lengthen RTs. Blue indicates negative weighting and red indicates positive weighting. **B.** Histogram of weighting values across the 3D d-SA matrix.

Table S1. Regional Distribution of d-SA Weighting Matrix

	Cluster Center (XYZ)			Voxel #	Average Weight
Brain Stem	43.46	47.72	30.39	158	0.15
Central Opercular Cortex	24.74	67.63	38.74	19	-0.22
Cingulate Gyrus, anterior division	44.58	76.14	48.54	440	0.08
Cingulate Gyrus, posterior division	45.11	43.92	48.63	546	-0.11
Cuneal Cortex	45.48	23.15	50.15	845	0.00
Frontal Operculum Cortex	24.00	72.66	37.04	187	0.11
Frontal Orbital Cortex	43.37	73.73	29.18	1017	0.00
Frontal Pole	30.22	85.63	50.15	474	-0.01
Inferior Frontal Gyrus opercularis	19.90	72.80	38.40	10	0.13
Inferior Frontal Gyrus triangularis	19.54	77.25	37.83	313	-0.07
Insular Cortex	32.31	69.87	34.02	450	0.03
Intracalcarine Cortex	44.83	26.16	40.21	1078	0.03
Lateral Occipital Cortex-inferior	41.67	27.08	42.13	86	-0.15
Lateral Occipital Cortex-superior	46.82	22.63	50.20	2279	-0.01
Left Hippocampus	56.92	49.67	29.38	24	-0.34
Lingual Gyrus	45.61	31.36	33.60	1247	0.00
Middle Frontal Gyrus	31.47	76.63	53.34	122	-0.16
Middle Temporal Gyrus-anterior	21.46	63.38	22.77	13	0.20
Middle Temporal Gyrus-posterior	19.11	53.76	28.85	112	-0.02
Occipital Fusiform Gyrus	50.72	22.52	27.84	90	-0.37
Occipital Pole	46.26	16.54	47.23	1446	0.04
Paracingulate Gyrus	44.03	80.84	49.78	585	0.03
Parahippocampal Gyrus	50.81	46.42	29.16	227	0.12
Planum Polare	24.43	60.59	27.48	54	-0.28
Postcentral Gyrus	53.31	41.80	61.38	81	-0.28
Precuneous Cortex	45.34	34.89	58.11	1985	-0.01
Right Thalamus	38.09	51.32	33.36	22	-0.11
Subcallosal Cortex	47.45	72.78	29.40	137	-0.09
Superior Frontal Gyrus	38.11	72.13	65.46	641	0.05
Superior Parietal Lobule	52.81	36.92	65.15	26	-0.04
Superior Temporal Gyrus-anterior	21.64	63.64	24.64	11	0.02
Superior Temporal Gyrus-posterior	20.44	53.62	32.15	39	0.33
Supracalcarine Cortex	42.75	29.20	43.55	176	0.13
Temporal Fusiform Cortex	53.84	45.33	22.84	69	0.20
Temporal Occipital Fusiform Cortex	49.58	37.13	28.96	262	-0.08
Temporal Pole	53.31	70.55	21.70	308	0.10

Table S2. Prediction of ICG Score from d-SA Expression with Covariates

	B	T	*p*	95% CI	*Partial Corr*
Months Since Loss	.83	1.42	.17	-0.38 to 2.05	0.31
Psychiatric Medication	3.53	.84	.41	-5.23 to 12.30	0.19
# MDD episodes	-.77	-.47	.64	-4.20 to 2.65	-0.11
Income	-.65	-.41	.68	-3.95 to 2.66	-0.09
d-SA Expression	-30.79	-2.46	.02	-56.95 to -4.62	-0.49

d-SA pattern expression during non-intrusion blocks predicts Inventory for Complicated Grief (ICG) score while controlling for demographic correlates of ICG.

Table S3. Prediction of ICG Score from d-SA Expression Controlling for Loss Type

	B	T	*p*	95% CI	*Partial Corr*
d-SA Expression	-29.68	-4.29	<.00	-44.02 to -15.34	-.67
Loss Type	12.56	3.91	<.00	5.89 to 19.24	.64

d-SA pattern expression during non-intrusion blocks predicts Inventory for Complicated Grief (ICG) score while controlling for type of loss (i.e. suicide vs non-suicide).

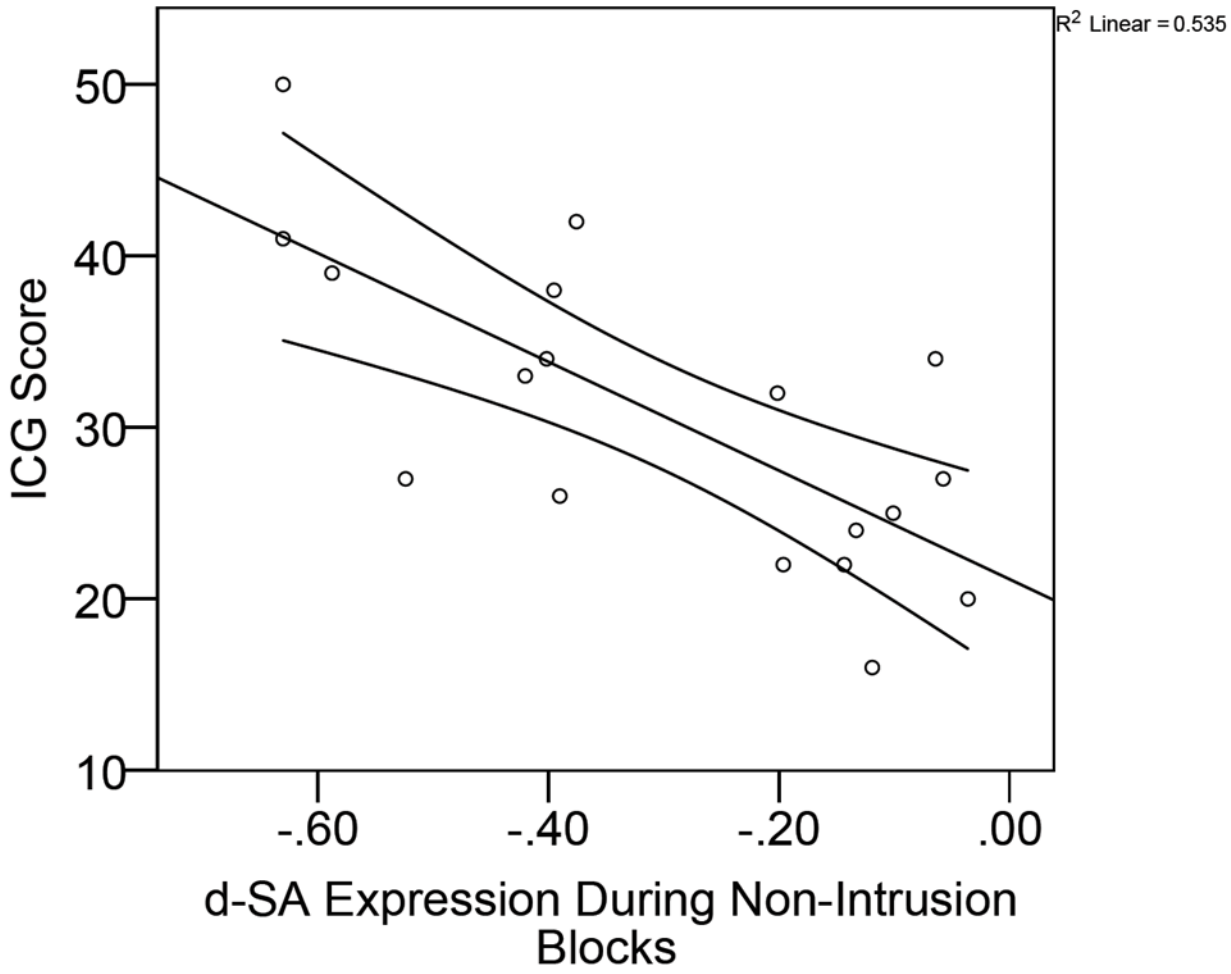

Figure S2. Grief Severity by d-SA Expression in Suicide Bereaved Only

Figure S3. Grief Severity by d-SA Expression in Original 23 Subjects

Supplemental References

1. Woolrich MW, Jbabdi S, Patenaude B, Chappell M, Makni S, Behrens T, et al. (2009): Bayesian analysis of neuroimaging data in FSL. *Neuroimage*. 45:S173-186.

2. Zhang Y, Brady M, Smith S (2001): Segmentation of brain MR images through a hidden Markov random field model and the expectation-maximization algorithm. *IEEE transactions on medical imaging*. 20:45-57.

3. Jenkinson M, Bannister P, Brady M, Smith S (2002): Improved optimization for the robust and accurate linear registration and motion correction of brain images. *Neuroimage*. 17:825-841.

4. J.L.R. Andersson MJaSMS (2007): Non-linear registration, aka Spatial normalisation. *FMRIB technical report TR07JA2*.

5. Conroy BR, Walz JM, Sajda P (2013): Fast bootstrapping and permutation testing for assessing reproducibility and interpretability of multivariate fMRI decoding models. *PloS one*. 8:e79271.